Exp Fluids (2007) 43:641–653
DOI 10.1007/s00348-007-0357-4

RESEARCH ARTICLE

Fish locomotion: kinematics and hydrodynamics of flexible foil-like fins

George V. Lauder · Peter G. A. Madden

Received: 12 February 2007 / Revised: 30 June 2007 / Accepted: 2 July 2007 / Published online: 22 July 2007

Abstract The fins of fishes are remarkable propulsive devices that appear at the origin of fishes about 500 million years ago and have been a key feature of fish evolutionary diversification. Most fish species possess both median (midline) dorsal, anal, and caudal fins as well as paired pectoral and pelvic fins. Fish fins are supported by jointed skeletal elements, fin rays, that in turn support a thin collagenous membrane. Muscles at the base of the fin attach to and actuate each fin ray, and fish fins thus generate their own hydrodynamic wake during locomotion, in addition to fluid motion induced by undulation of the body. In bony fishes, the jointed fin rays can be actively deformed and the fin surface can thus actively resist hydrodynamic loading. Fish fins are highly flexible, exhibit considerable deformation during locomotion, and can interact hydrodynamically during both propulsion and maneuvering. For example, the dorsal and anal fins shed a vortex wake that greatly modifies the flow environment experienced by the tail fin. New experimental kinematic and hydrodynamic data are presented for pectoral fin function in bluegill sunfish. The highly flexible sunfish pectoral fin moves in a complex manner with two leading edges, a spanwise wave of bending, and substantial changes in area through the fin beat cycle. Data from scanning particle image velocimetry (PIV) and time-resolved stereo PIV show that the pectoral fin generates thrust throughout the fin beat cycle, and that there is no time of net drag. Continuous thrust production is due to fin flexibility which enables some part of the fin to generate thrust at all times and to smooth out oscillations that might arise at the transition from outstroke to instroke during the movement cycle. Computational fluid dynamic analyses of sunfish pectoral fin function corroborate this conclusion. Future research on fish fin function will benefit considerably from close integration with studies of robotic model fins.

G. V. Lauder (✉) · P. G. A. Madden
Museum of Comparative Zoology,
Harvard University, 26 Oxford Street,
Cambridge, MA 02138, USA
e-mail: glauder@oeb.harvard.edu

1 Introduction

Of the most prominent characteristics of early fossil fishes are the median and paired fins that project from the body surface into the surrounding fluid. Fins have been a fundamental design feature of fishes since their origin ~500 million years ago, predating even the origin of jaws and the ability of early fishes to bite and chew food. The subsequent evolutionary diversification of fishes into over 28,000 species has been marked by differentiation of distinct midline and paired fin structures and the evolution of complex skeletal supports and control musculature for these fins (Lauder 2006). Most fishes possess median (midline) dorsal, anal, and caudal (tail) fins, as well as paired pectoral and pelvic fins (Fig. 1) for a total of seven discrete control surfaces in addition to the body surface. Fish fins play a prominent role in the control of body position and stability and in generating locomotor forces during propulsion and maneuvering. But the vast majority of the work to date on fish propulsion has focused on the body surface. Patterns of body deformation during locomotion and their hydrodynamic effect have been well described (reviewed in Fish and Lauder 2006; Lauder and Tytell 2006), as has the arrangement of body musculature and the activity and contractile characteristics of these

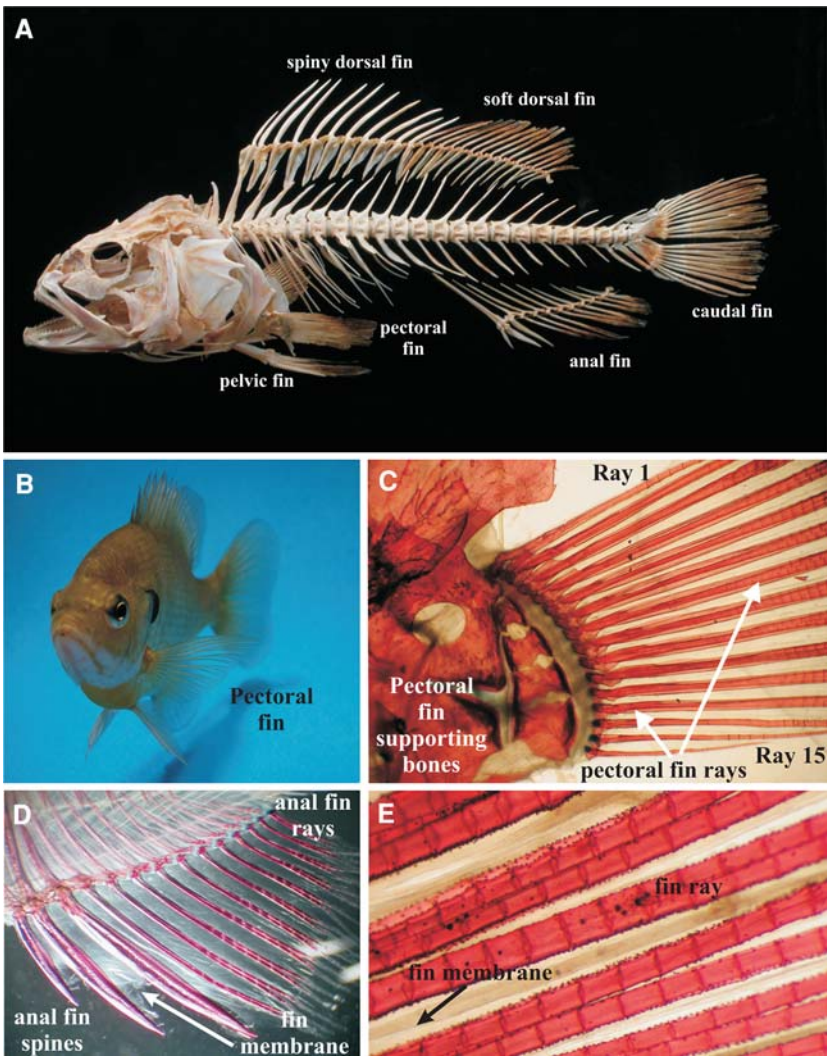

Fig. 1 Structure of the fin skeleton in bony fishes. **a** Snowy grouper, *Epinephelus niveatus*, skeleton showing the positions of the paired and median fins and their internal skeletal supports. Note that each of the median fins has segmented bony skeletal elements that extend into the body to support the fin rays and spines, and that muscles controlling the fin rays arise from these skeletal elements. **b** Bluegill sunfish, *Lepomis macrochirus*, hovering in still water with the left pectoral fin extended. **c** Structure of the pectoral fin and the skeletal supports for the fin; bones have been stained *red*. This specimen had 15 pectoral fin rays that articulate with a crescent-shaped cartilage pad (*tan color*) at the base of the fin. The smaller bony elements to the left of the cartilage pad allow considerable reorientation of the fin base and hence thrust vectoring of pectoral fin forces (Drucker and Lauder 1999, 2003). **d** Anal fin skeleton (bones stained red and muscle tissue digested away) to show the three leading spines anterior to the flexible rays, and the collagenous membrane that connects adjacent spines and rays. **e** Close view of pectoral fin rays (*stained red*) to show the segmented nature of bony fish fin rays and the membrane between them. Images in panels A and B modified from Lauder et al. (2007)

muscles (Shadwick and Gemballa 2006; Syme 2006). And computational fluid dynamic analyses of body movement (Carling et al. 1998; Kern and Koumoutsakos 2006; Ramamurti et al. 1999; Wolfgang et al. 1999; Zhu et al. 2002) have recently provided new insights into how body deformation generates wake-flow patterns and force production to power movement.

Studying fish fin structure and function is critical to understanding how fish maintain stability and generate force during propulsion and maneuvering, especially in locomotor gaits during which fins are the only propulsive surfaces active and the body is not used (Drucker and Lauder 2000). And yet fins have been subject to only relatively limited experimental study until recently. In this paper we first present a brief general overview of recent experimental studies on fish fin kinematics and hydrodynamics, and then provide new experimental data on the hydrodynamic function of fish pectoral fins obtained using both scanning particle image velocimetry (PIV) and stereo PIV in freely swimming fish.

2 Overview of fish fin structure and function

Fish fins are supported by flexible bony or cartilaginous fin rays that extend from the fin base into the fin surface and provide support for the thin collagenous membrane that connects adjacent fin rays (Figs. 1, 2). Fin rays articulate with the fin skeleton located inside the body wall which supports musculature that allows the fin rays to be actively moved from side to side and elevated and depressed (Fig. 1, Geerlink and Videler 1974; Geerlink 1979; Jayne et al. 1996; Winterbottom 1974). Many fish also have dorsal and anal fins which have leading spiny portions of the fin (Fig. 1, Drucker and Lauder 2001b), and fin spines typically can only be elevated and depressed; they possess limited sideways mobility. The posterior region of the dorsal and anal fins is known as the "soft" dorsal or anal fin and is supported only by flexible fin rays. Recordings from fin musculature, which is distinct from the body muscles, unequivocally show that fins are actively moved during swimming, and that this active movement generates a vortex wake that passes downstream toward the tail, which thus intercepts the flow that is greatly altered from the free-stream (Drucker and Lauder 2001b, 2005; Jayne et al. 1996; Standen and Lauder 2007) (also see Fig. 4). The modulus of elasticity of bony fin rays is about 1 GPa, while the membrane in between fin rays has a modulus of about 0.3–1.0 MPa (Lauder et al. 2006).

The hallmark of fish fin functional design is the bending of the fin rays which permits considerable flexibility of the propulsive surface. The fin rays of the large fish group termed ray-finned fishes (but not sharks), possess a remarkable bilaminar structure and muscular control that allows fish to actively control fin surface conformation and camber during locomotion. As illustrated in Fig. 2, each bony fin ray is composed of two halves (termed hemitrichs) which are connected along their length by short collagen fibers and may be attached at the end of the ray (Alben et al. 2007; Geerlink and Videler 1987; Lauder 2006). Each fin ray is actuated by four separate muscles, and thus a single fin such as the pectoral fin of a bluegill sunfish (*Lepomis macrochirus*), which has about 14 fin rays, potentially has over 50 separate actuators that allow the fin to be reoriented in three dimensions with control over the position of each ray. Neural control of fin ray motion has yet to be studied in detail, and the extent to which anatomically homologous muscles on neighboring fin rays can be controlled independently is unknown. Most importantly, displacement of the two ray halves through the contraction of fin ray musculature at the base of the fin causes the fin ray to curve. Fish can thus actively alter the conformation of their propulsive surface by actively bending fin rays, and can resist hydrodynamic loading, a phenomenon that is observed most clearly during maneuvering (Fig. 2d). One result of the complex control and bilaminar fin ray design

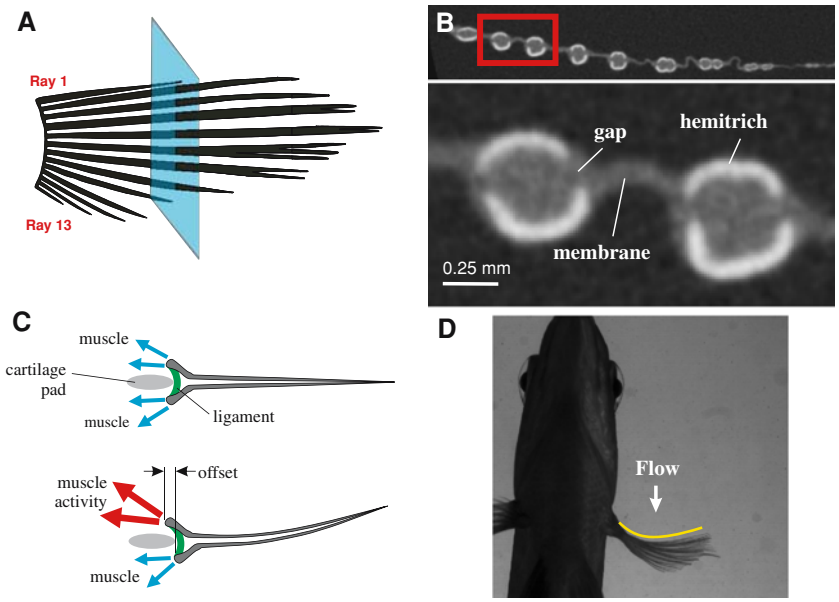

Fig. 2 Pectoral fin structure in bluegill sunfish, *Lepomis macrochirus*. **a** Schematic view of the pectoral fin which typically has 12–15 fin rays. **b** Cross-section through fin rays at the level of the *blue* plane shown in panel A obtained with μCT scanning (see Alben et al. 2007) in which bone is *whitish* color, and fin collagen and membrane are *gray*. Cross-sectional image of rays (*top*) and close view of two adjacent rays (*below*). Each fin ray is bilaminar, with two curved half rays termed hemitrichs. **c** Schematic of the mechanical design of the bilaminar fin ray in bony fishes. Each fin ray has expanded bony processes at the base of each hemitrich to which muscles attach (*blue arrows*). Differential actuation of fin ray muscles (*red arrows*) results in curvature of the fin ray. Fish can thus actively control the curvature of their fin surface. **d** Frame from high-speed video of a bluegill sunfish during a turning maneuver, showing the fin surface (outlined in *yellow*) curving *into* oncoming flow

in fish fins is that, as illustrated in Sect. 5, fins can undergo rather complex three-dimensional changes in shape during locomotion.

3 Methodology for experimental analyses of fish locomotion

Although experimental kinematic and hydrodynamic studies of fishes swimming in large bodies of water and under natural settings would be ideal, recent progress in understanding the functional design of fishes has relied heavily on inducing locomotion in laboratory flow tanks, which permit precise speed control and the induction of replicated maneuvering stimuli. Such studies have allowed both detailed kinematic studies of fin function and experimental hydrodynamic recordings of wake flow patterns resulting from fin and body movement using PIV (e.g., Anderson 1996; Drucker and Lauder 1999, 2002a; Lauder and Drucker 2002, 2004; Liao et al. 2003; Nauen and Lauder 2002a, b; Wilga and Lauder 2002; Wolfgang et al. 1999).

Two critical enabling technologies that have been responsible for considerable progress in understanding fish locomotor function in recent years are (1) the use of high-resolution (at least megapixel) high-speed video cameras acquiring images between 200 and 1000 frames per second or more, and (2) the use of time-resolved PIV (Lauder and Madden 2008). Often these two techniques are used in conjunction with other approaches such as electrical recordings of fin and body muscle activity patterns and measurement of muscle strain (e.g., Lauder et al. 2006), or the use of biorobotic fish-like devices that enable precise control of kinematics and exploration of broad (and even non-biological) parameter spaces (Lauder et al. 2007). The rapid development of high-speed digital video technology over the past decade coupled with the availability of lower cost continuous wave lasers has also permitted their use in PIV studies by biologists. This has allowed time-resolved PIV (typically at 200–1,000 Hz) recordings of fin and body wake flows with a temporal resolution 10–50 times that of the fin beat frequency, giving a detailed picture of vorticity production and the generation of biological flows near the body and fins (Drucker and Lauder 1999, 2002a, 2003; Lauder 2000; Lauder and Drucker 2004). Megapixel high-speed video cameras have made the motion of individual fin rays visible (see Fig. 5, for example) and have permitted the accurate quantification of fin surface conformation (especially the bending of individual fin rays) which is critical to interpreting the kinematic causes of wake flow patterns.

One critical issue in experimental fluid dynamic studies of freely swimming fishes is that the position of the fish in the laser light sheet used for PIV must be known. Wake flow patterns produced by swimming fishes are highly sensitive to the location of the PIV light sheet, since the three-dimensional structure of the wake changes substantially with height on the body, and wake flows from dorsal and anal fins change the flow structure substantially above and below the tail (Standen and Lauder 2007; Tytell 2006). Thus, we highly recommend the use of multiple high-speed cameras to image simultaneously fin kinematics, wake flow patterns, and body position in the laser light sheet. Figure 3a shows an image of a brook trout swimming in a recirculating flow tank with dual light sheets generated by two argon–ion continuous wave lasers to study dorsal and anal fin function. Simultaneous use of multiple orthogonal high-speed video cameras allows imaging the wake flows from both the dorsal and anal fins at the same time, as well as fin and body position relative to the light sheets. Inducing fish to swim in such a restricted position in the flow tank can be difficult and time-consuming, but careful selection of sequences and accurate fish positioning is vital to obtaining accurate data on fin hydrodynamic function.

While time-resolved two-dimensional PIV with high-speed cameras and continuous lasers has been used to study fin function in several species of fishes to date (Drucker and Lauder 2000, 2003; Liao and Lauder 2000; Müller et al. 2000; Nauen and Lauder 2002a; Tytell 2004; Tytell and Lauder 2004; Wilga and Lauder 1999, 2000, 2001), three-dimensional information on fish fin flow patterns is highly desirable. Such data can be obtained in part by using stereo PIV (Nauen and Lauder 2002b) or using multiple light sheet orientations (Drucker and Lauder 1999), but even this approach only generates the three vector components of flow confined to one or more narrow (1–2 mm thick) planes. Reconstructions of three-dimensional flow patterns then requires piecing together data from several different fin beat cycles which is difficult as freely swimming fishes often do not move their fins in precisely the same manner from stroke to stroke or maintain strict control of body position. Phase averaging of fin PIV data from freely swimming fishes is possible (e.g., Tytell and Lauder 2004) but often difficult to do without introducing considerable variation into the data.

In Sect. 6 below we describe data obtained on the hydrodynamics of the bluegill sunfish pectoral fin using both scanning PIV, and a transverse-plane PIV approach that samples flow with high temporal resolution downstream of swimming fish with cameras that view the wake from behind (Fig. 3). These approaches, especially when used in conjunction with each other, provide a reasonably complete picture of fin-induced three-dimensional flow patterns.

In scanning PIV, a continuous wave horizontal light sheet is scanned, using a moving mirror, down through the

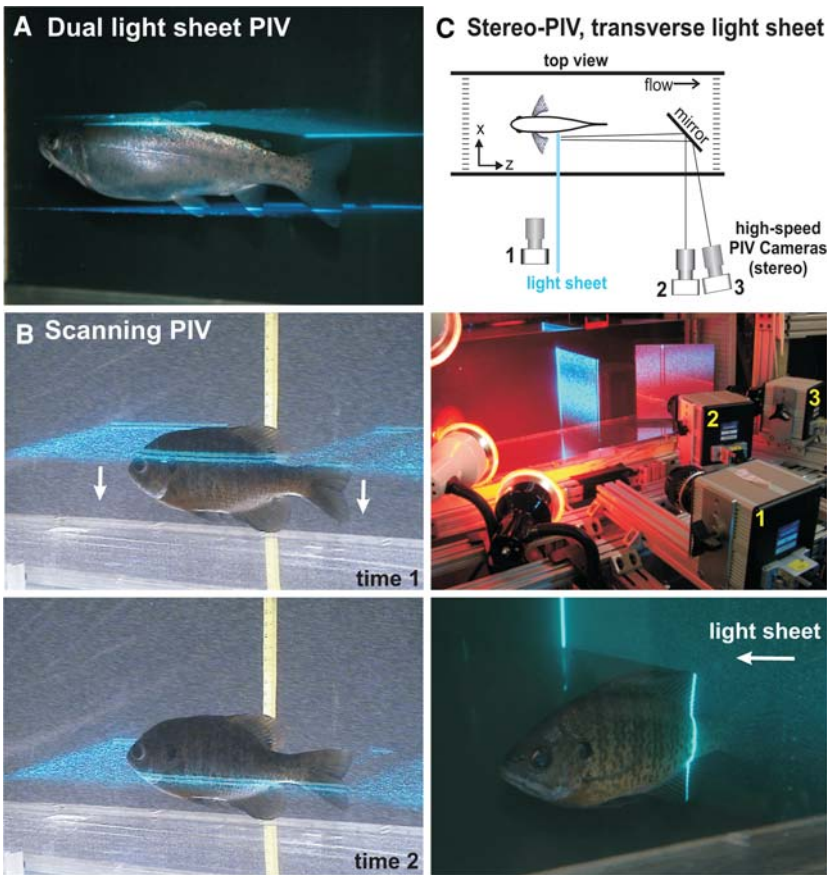

Fig. 3 Methods for the study of fin hydrodynamics in freely swimming fishes. **a** Brook trout swimming between two light sheets produced by two continuous wave argon–ion lasers to study the function of dorsal and anal fins. High-speed digital video cameras image the fin wake flow patterns from above and below at the same time. Image by E. Standen, from Standen and Lauder (2007). **b** Scanning PIV in which a horizontal laser light sheet is rapidly scanned vertically through the beating pectoral fin (*white arrows* indicate the direction of laser sheet movement) in freely swimming bluegill sunfish to image fin wake flow patterns. **c** Experimental arrangement for stereo PIV using a light sheet transverse to swimming bluegill, downstream of the beating pectoral fin. *Top panel* shows a schematic top view of the experimental arrangement. Use of three high-speed cameras allows simultaneous imaging of body and fin position (camera 1) and stereo PIV of flow through the transverse light sheet (*middle panel*, camera #2 and #3). These two cameras were aimed at a mirror downstream of the swimming fish, imaging at 500 Hz, 1/2,000 s shutter speed, and provided data on the u, v, and w components of flow through the transverse laser light sheet. The *bottom panel* shows a bluegill swimming in the flow tank with the transverse light sheet. Bluegill swam with their pectoral fin at varying distances upstream of the light sheet in different trials (*bottom panel* image courtesy of E. Tytell)

moving pectoral fin and its wake (Fig. 3b). The light sheet scans through 5–10 cm vertical distance in 50–100 ms, and particle flows are imaged with a high-speed camera (1,024 × 1,024 pixel resolution) at 500 Hz from below the light sheet looking up at the fish and the fin wake. A side-view camera provides data on the position of the light sheet relative to the fish fin, and gives basic kinematic data on the motion of the fin. Brucker (1997), Rockwell et al. (1993), and Burgmann et al. (2006) provide further discussion of PIV scanning approaches.

In another set of experiments, we used a continuous laser light sheet oriented transversely to the fish body axis and placed downstream of the fish fin (Fig. 3c). Fin wake flows move toward and then through the laser light sheet as the fish maintains position in the flow tank while swimming at a slow pectoral fin swimming speed. With a temporal sampling rate of 500–1,000 Hz and short shutter speeds (1/2,000 s or less), stereo PIV images can be obtained of wake flow patterns moving toward the camera, and reconstructed into a three-dimensional representation of fin flows. Brücker (2001) discusses PIV using a light sheet orientation orthogonal to free-stream flow and issues involved in imaging such flows from downstream. This approach has the advantage of imaging the full wake from the body surface to a distance of several fin chords away into the free-stream as flow moves into the transverse light sheet. An additional feature of these experiments is the use of another camera to image fish body position in a side view (Fig. 3c),

allowing quantification of fish body acceleration during the fin beat synchronously with the stereo PIV images. As shown in Fig. 3c, we used red light to illuminate the swimming fish, and a Photron PCI 1024 high-speed digital video camera with a highpass filter on the lens to allow red light through but block green light from the continuous wave argon–ion laser. This camera (#1 in Fig. 3c) imaged body position and fin movement. Two additional identical synchronized Photron cameras (#2 and #3 in Fig. 3c) were aimed in stereo configuration with Scheimpflug adapters at a mirror in the flow tank downstream from the swimming fish. These two cameras were focused onto the laser light sheet located upstream of the mirror (Fig. 3c) and had lowpass filters on each lens to block red light but allow the green light from the argon–ion laser through to the camera sensors. This experimental arrangement allows simultaneous acquisition of body and fin position through time and fin wake flows in stereo view. Since fin wake flows advect through the laser plane, a three-dimensional view of the fin wake can be formed. However, since the wake is sampled at only one location, any interactions among vortices downstream of the laser plane will not be visualized. All camera views were calibrated and u, v, and w velocity vector components calculated using Davis 7.1.1 software from LaVision Inc., Ypsilanti, MI, USA. Multiple replicate experiments were conducted on individual bluegill sunfish (*Lepomis macrochirus*) of mean total body length (L) of 18 cm swimming at 0.5 Ls^{-1}. Swimming bluegill naturally positioned themselves at slightly different positions in the flow tank during the replicate trials, and thus data were obtained with the fin at different distances upstream of the transverse light sheet. In most sequences, the posterior region of the body can be seen in the PIV views as the tail extends toward the PIV cameras (Figs. 3c, 7a, 8). PIV sequences of the pectoral fin wake were obtained of steady swimming and also a variety of maneuvers, but in this paper we focus on the steady swimming data. These experimental analyses are conducted in conjunction with computational fluid dynamic analyses of sunfish pectoral fin function (Lauder et al. 2006; Mittal et al. 2006).

4 Overview of dorsal and anal fin function

In this section we present kinematic and hydrodynamic data from fish dorsal and anal fins to illustrate the extent to which flows generated by these fins modify the hydrodynamic environment experienced by the tail, and as an example of the hydrodynamics of median fin function.

Perhaps the most surprising result to emerge from analyses of fish dorsal and anal fin function to date is the extent to which these fins generate side forces. Analyses of median fin wake flows in both trout and sunfish (Drucker and Lauder 2001b, 2005; Standen and Lauder 2005, 2007) show that although a reasonable amount of thrust may be produced, the majority of locomotor force produced by median fins is directed laterally, to each side (Fig. 4). In bluegill sunfish, the soft dorsal fin generates about one-third of the thrust produced by the tail, and approximately twice as much lateral force as thrust. Tytell (2006) estimated that together, the dorsal and anal fins in bluegill generate nearly as much total force as the tail fin. But in rainbow trout, Drucker and Lauder (2005) showed that the dorsal fin generates side forces that are five times thrust force magnitudes, and that the dorsal fin produces a distinct vortex wake at swimming speeds less than 2.0 body lengths (L) per second. Figure 4a illustrates the vortex wake of the dorsal fin of a rainbow trout swimming at 1 Ls^{-1}. Strong pulses of fluid momentum directed to each side are generated as the

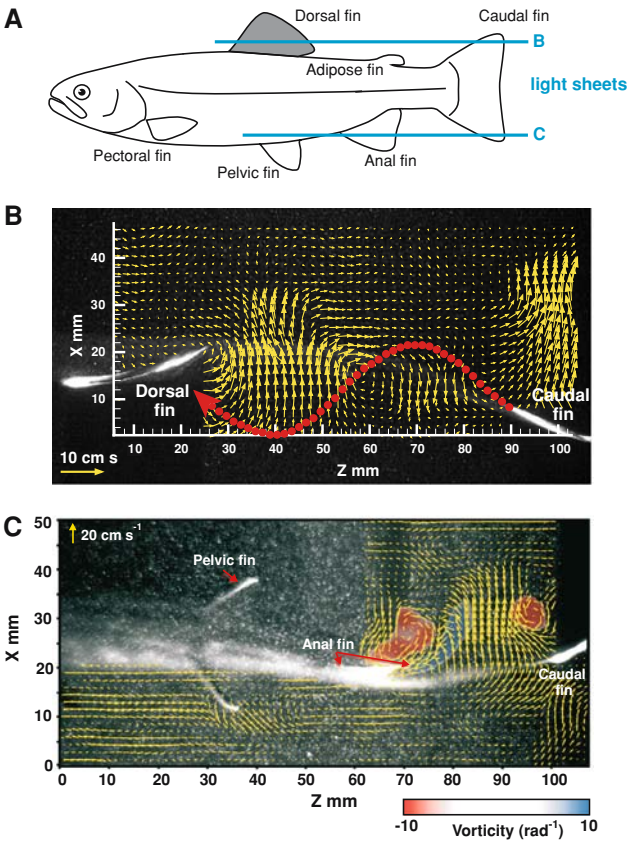

Fig. 4 Median fin hydrodynamics in swimming trout. **a** Schematic to show the position of dorsal and anal fins in trout and the position of the laser light sheets in panels B and C. Trout have an additional small median fin, the adipose fin, that is not actively moved. **b** Dorsal fin wake (*yellow arrows*) in rainbow trout swimming steadily at 1.0 Ls^{-1}. The dorsal fin is to the left and the tail to the right. Note the alternating lateral jet flows shed by the dorsal fin. The *red dots* show the path of the tail, which moves through the centers of vortices shed by the dorsal fin (from Drucker and Lauder 2005). **c** Anal fin wake from a brook trout swimming steadily at 0.5 Ls^{-1}. Strong lateral momentum is shed into the wake by the anal fin, and the tail moves through this vortex wake (from Standen and Lauder 2007)

dorsal fin sweeps back and forth, and the tail passes through the centers of the shed vortices. At higher swimming speeds above 2.0 Ls^{-1}, however, dorsal fin amplitude decreases and no wake is formed: the dorsal fin is most active during slow swimming and appears to be inactive during more rapid locomotion (Drucker and Lauder 2005).

Standen and Lauder (2007) studied the function of both dorsal and anal fins in swimming brook trout, and found that both fins generate significant wake vorticity that is directed to the same side of the fish resulting in balanced roll torques (Fig. 4b). Neither the dorsal nor the anal fins generate significant thrust, while both fins produce nearly synchronous side momentum jets even though the dorsal and anal fins are located at different longitudinal positions on the trout. Differences in dorsal and anal fin shape and heave and pitch motions combine to result in temporally coincident jet formation which in turn balances roll torques.

The observation that the caudal fin moves through the dorsal and anal fin wake suggests that, if the motion of the caudal fin is phased appropriately, additional thrust may be obtained resulting from the increase in angle of attack at the tail that results from the change in free-stream flow generated by the dorsal and anal fins (Drucker and Lauder 2001b; Standen and Lauder 2007). Computational fluid dynamic analysis of two foils in series using the pattern of motion from the sunfish dorsal fin and tail (Akhtar et al. 2007), showed that indeed considerable increases in thrust are realized by the sunfish tail as a direct result of the dorsal fin wake initiating the formation of a stronger leading edge vortex on the tail than would otherwise be present. Interestingly, the phase difference between the sunfish dorsal fin and tail (108°) was not the optimal phase possible. Exploration of the phase parameter space showed that a phase of 48° produced optimal thrust enhancement by the tail, although this is a phase relationship never seen in a swimming sunfish due to the coupling between the dorsal fin and tail through the body.

Experimental data on median fin hydrodynamics in fishes (Fig. 4) indicate that the these fins play a substantial role in the maintenance of body stability, in modifying the flow environment encountered by the tail, and, in the case of sunfish, generating thrust during steady rectilinear propulsion. There is a considerable diversity of median fin structure in fishes, and yet the hydrodynamic significance of this variation is as yet unknown, and there are a plethora of questions for future experimental hydrodynamic research on the median fins of fishes.

5 Pectoral fin function: kinematics

A conspicuous feature of biological propulsion in fluids (especially water) is flexibility of the thrust-generating surfaces, and bending and twisting of control surfaces is especially evident when fishes swim at slow speeds using only their fins (and not body deformation) to produce thrust. In particular, the pectoral fin swimming gaits of bluegill sunfish (Fig. 5) illustrate how fish fins deform during propulsion, and the complexity of this deformation. When swimming steadily at slow speeds (less than 1 Ls^{-1}), bluegill sunfish use the paired pectoral fins almost exclusively. On the outstroke, both the upper and lower edges of the fin move away from the body wall in a nearly simultaneous motion which results in the fin achieving a "cupped" configuration (Fig. 5b, e): the pectoral fin has two leading edges. Fin area increases during the outstroke, and the upper third of the fin bends into a wave that travels spanwise from fin root to tip at a speed faster than the swimming speed: hence this traveling wave along the upper fin margin appears to contribute to thrust. The maximum "cupped" configuration is achieved at about 75% of the outstroke as the upper and lower fin edges move toward each other. Minimum fin area occurs at the time the fin transitions from the outstroke to the return stroke.

Early in the retraction stroke of the pectoral fin, the upper fin wave has progressed nearly two-thirds of the way along the fin span and causes a "dimpling" of the fin surface behind the upper edge (Fig. 5f) which appears to stabilize the vortex formed on the upper fin edge (Lauder et al. 2006). On the return or retraction stroke, fin area increases and the fin moves rapidly back to lie flat along the body. There is often an extended time in between fin beats during which the fin is held along the body wall (Gibb et al. 1994) before the next beat begins.

Pectoral fin kinematics in bluegill sunfish are broadly representative of how many bony fishes use their pectoral fins using a complex and time-varying combination of lift-and-drag forces to generate thrust. But some species exemplify more clearly the ends of the lift-and-drag continuum, and use primarily drag-based propulsion (Walker 2004) or lift-based mechanisms (Walker and Westneat 1997).

Fin kinematics during maneuvering locomotion are substantially different from propulsion, and may involve much more substantial bending of fin rays, greater angular excursions, and dramatic differences between pectoral fin conformation on the left and right sides of the body during a turn (Drucker and Lauder 2001a; Higham et al. 2005; Lauder et al. 2006). This contrasts with patterns of wing motion in birds and insects where left–right differences in wing kinematics during turns are relatively slight (Dickinson 2005; Warrick et al. 1998).

6 Pectoral fin function: hydrodynamics

Given the complex deformation and movement of fish pectoral fins, it is perhaps not surprising that the flows

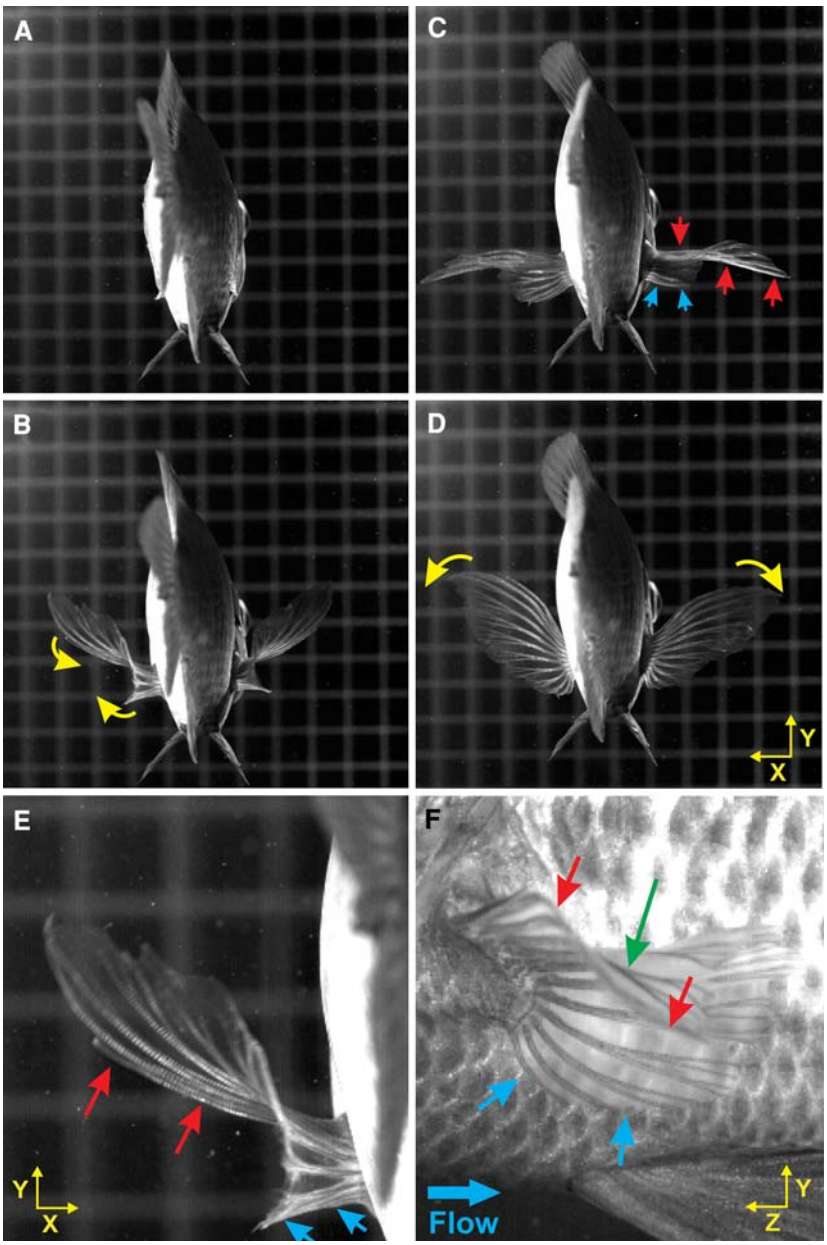

Fig. 5 Pectoral fin kinematics in bluegill sunfish (18 cm *L*) swimming at 0.5 Ls^{-1}. Panels A–D show four times during a single fin beat cycle. Images are from 250 Hz digital video (1,024 × 1,024 pixel resolution) taken from behind the swimming bluegill looking upstream. *Yellow arrows* show the major movement patterns of the fin, while *red* and *blue arrows* point to the upper (*dorsal*) and lower (*ventral*) margins of the fin, respectively. **a** Pause phase when the pectoral fin is held against the body, prior to the start of the fin beat cycle. **b** Middle of the fin outstroke ("downstroke") showing the cupped configuration of the fin in which both the upper and lower fin rays move out from the body together, forming two leading edges. **c** Twisting of the fin at the transition between outstroke and return stroke. **d** Middle of the return stroke ("upstroke") during which the fin is expanded and pulled back toward the body (axis labels in this panel apply to panels A–D). **e** Enlarged view of the fin at the position shown in panel B to show details of the cupped fin conformation and the positions of the individual fin rays. **f** Enlarged view of the fin in side view slightly prior to the image in panel C to show the wave of bending that passes out the upper third of the fin from root to tip. Note the "dimple" formed behind the upper edge of the fin (*green arrow*) and variation in conformation of the different fin rays at this time

induced by fin motion can also be complex. PIV has been used to understand the hydrodynamic effect and force production of pectoral fin movement during both propulsion and maneuvering in a diversity of fishes (sharks, sturgeon, bluegill sunfish, and trout, Drucker and Lauder 1999, 2000, 2001a, 2002b, 2003; Lauder et al. 2006; Wilga and Lauder 1999, 2000, 2001), but these studies have to date relied on more traditional PIV approaches using

two-dimensional laser light sheets, usually oriented horizontally (perpendicular to the body axis) or vertically (parallel to the fish body). Two useful modifications to the traditional PIV approach (Fig. 3) are (1) to scan a laser light sheet through the pectoral fin and its wake, and (2) to use a light sheet in a transverse, orthogonal orientation to free-stream flow and image flow from downstream. Both the modifications of the usual PIV approach provide increased three-dimensional information on the hydrodynamic consequences of fin function.

Scanning PIV of the bluegill sunfish pectoral fin wake (Fig. 6) demonstrates that during the fin outstroke (when it is moving away from the body), water is accelerated both downstream and laterally, to the side. Because the fin is translucent, flow structures can be resolved in between the fin and the body, and water between the body and fin is accelerated on the outstroke (also see Lauder et al. 2006). At the end of the outstroke (Fig. 6b) a vortex ring has been shed with a central momentum jet directed back and to the side. As the pectoral fin returns to the body on the instroke, a vortex loop is shed (Fig. 6c). There is a significant change in direction (nearly 90°) between the side momentum added to the water on the outstroke and the return stroke of the fin which is clearly evident in the wake shown in Fig. 6c.

Analysis of pectoral fin hydrodynamics using transverse plane stereo PIV (Fig. 7) shows that on the fin outstroke a large volume of water is accelerated beyond free-stream even though much of the fin is moving away from the body. Kinematic analysis (Fig. 5b) shows that on the outstroke the upper third of the fin is oriented down and back, and this region of the fin could thus generate thrust during the outstroke (Fig. 7).

Transverse plane PIV at the level of the pectoral fin shows that on the fin downstroke (data not shown here), the kinematic cupping of the fin in which both the upper and lower fin rays move away from the body simultaneously (Fig. 5b), produces dual leading edge vortices (Lauder et al. 2006). The simultaneous presence of opposite sign vortices on the pectoral fin may act to minimize vertical body oscillations compared to a heaving and pitching foil in which significant momentum is added to the water orthogonal to the free-stream on each half stroke.

On the instroke (Fig. 8), flow moves back toward the body and is directed initially down and medially, and later in the instroke almost directly medially. Throughout the instroke, a large region of flow is accelerated beyond free-stream (Fig. 8).

Figure 9 shows the result of calculations of momentum flux through the transverse laser plane to give single fin forces resolved throughout one fin beat cycle. Vertical and side forces generated by the fin average between 1 and

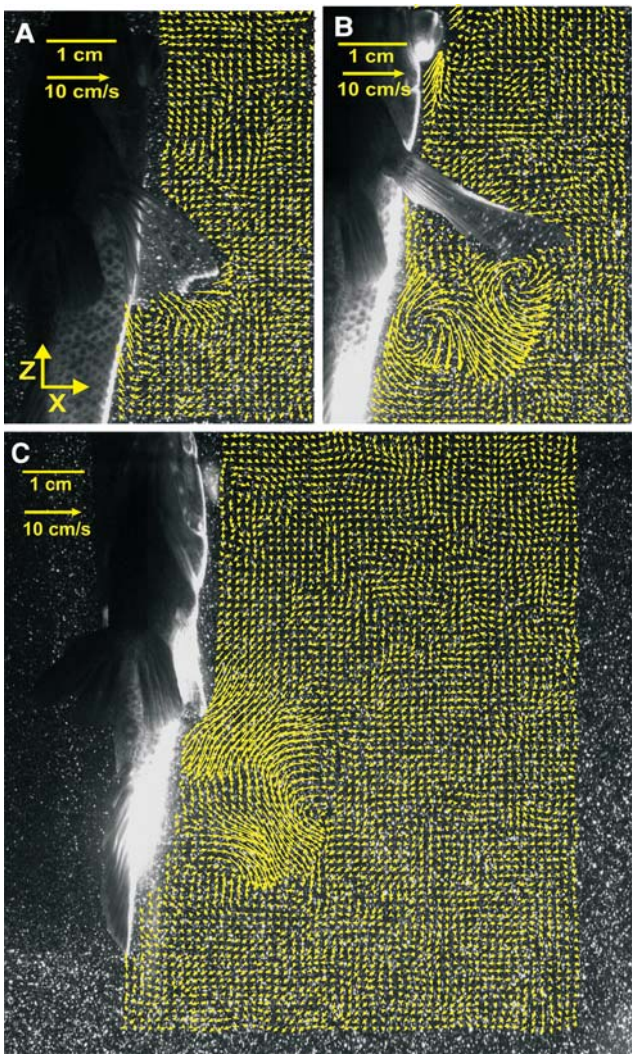

Fig. 6 Scanning PIV results from pectoral fin locomotion in a bluegill sunfish (L = 18 cm) swimming at 0.5 Ls^{-1} (see Fig. 3b for methods). The laser light sheet scanned from top to bottom, and wake flows were imaged from below at 500 Hz. Images show the wake flow patterns early in the fin outstroke (**a**), at the transition from outstroke to instroke (**b**), and after the fin has reached the body surface at the end of the instroke (**c**). Mean free-stream flow has been subtracted. Note especially the added momentum in the downstream and side directions on the fin outstroke, and the reversal of momentum seen in panel C between the outstroke and instroke, visible as the two nearly orthogonal regions of jet flow downstream of the pectoral fin. Axes in panel A apply to all panels

5 mN and there is only a small deviation from the initial values at the start of the beat. Fish often drift slightly during pectoral fin propulsion, and hence side and vertical forces may not return exactly to their initial values. Thrust force per fin peaks at about 2 mN, and the fin clearly generates thrust throughout the beat (Fig. 9c). Some temporal smoothing in the force trace may result from the fact that the transverse laser light sheet was ~0.5 L downstream from the pectoral fin.

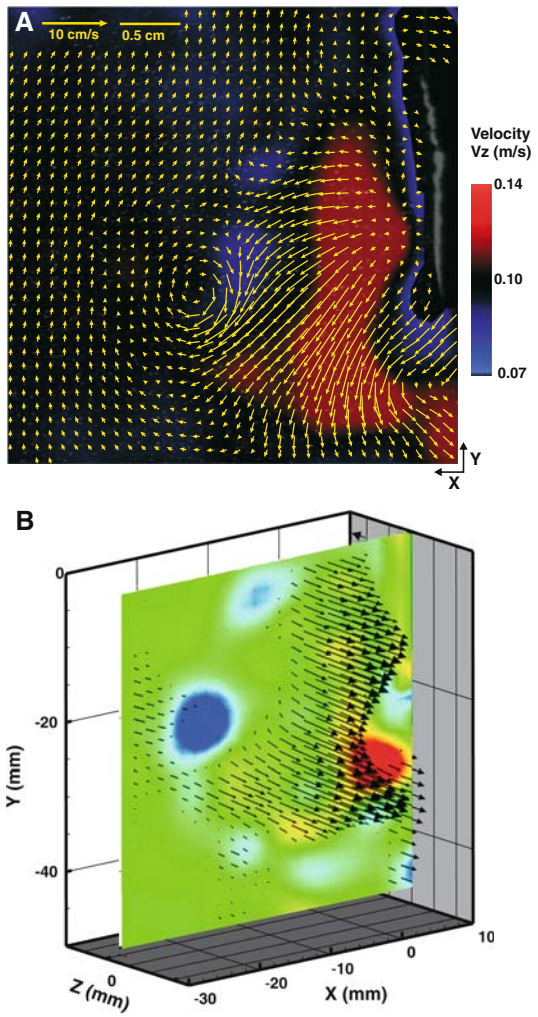

Fig. 7 PIV data imaged in the transverse plane (see Fig. 3c for methods) looking upstream at the wake shed by the pectoral fin of bluegill sunfish during locomotion at 0.5 Ls^{-1}. This figure shows data from the fin near the end of the outstroke. **a** Water velocity in the *xy* plane showing the u and v components of flow, with the w component (*z*-direction) illustrated as a contour plot in the background. *Red color* indicates water moving faster than mean free-stream flow (9 cm s^{-1}) as a result of pectoral fin motion, while *blue* indicates flow slowed to less than free-stream. The tail extends toward the camera in the middle right of the image, and vectors near the tail have been masked. Note the large region of *red* indicating that the pectoral fin outstroke has accelerated water in the wake to beyond free-stream velocity. **b** Three-quarter view of the pectoral fin wake flow at the same time as in panel A to show vorticity and velocity greater than free-stream. *Green color* indicates zero vorticity, blue negative vorticity (maximum 10 s^{-1}), and *red* positive vorticity (maximum 20 s^{-1}). Note the two counter rotating centers of flow separated by fluid accelerated beyond free-stream

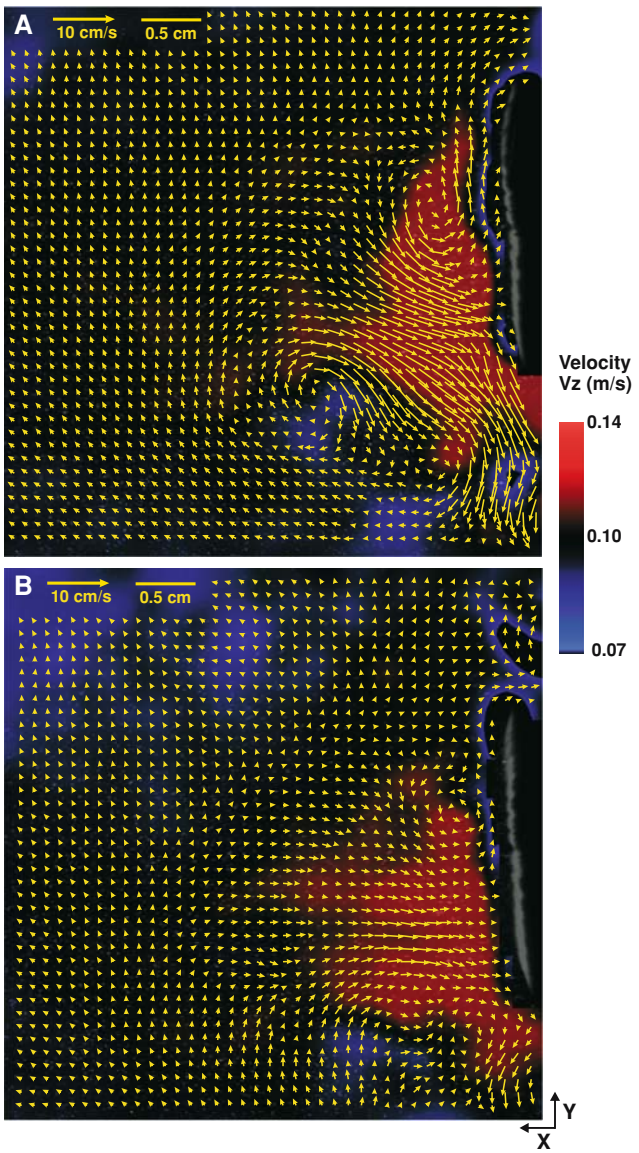

Fig. 8 PIV data imaged in the transverse plane (see Fig. 3c for methods) looking upstream at the wake shed by the pectoral fin of bluegill sunfish during locomotion at 0.5 Ls^{-1}. This figure shows data from the fin at mid-instroke (**a**) and late instroke (**b**). In both panels water velocity is shown in the *xy* plane (u and v components) of flow, with the w component (*z*-direction) illustrated as a contour plot in the background. *Red color* indicates water moving faster than mean free-stream flow (9 cm s^{-1}) as a result of pectoral fin motion, while *blue* indicates flow slowed to less than free-stream. The tail extends toward the camera in the middle right of the images, and vectors near the tail have been masked. **a** Note the change in direction of side velocity compared to the fin outstroke in Fig. 7 and the large region of accelerated flow. **b** Late in the instroke the pectoral fin wake is oriented toward the body and a region of accelerated flow is still evident

This pattern of pectoral fin thrust production measured experimentally in sunfish is consistent with that calculated using CFD based on sunfish pectoral fin kinematics (Mittal et al. 2006): the pectoral fin generates thrust throughout the fin beat. This result contrasts with data from many previous experiments and computational work on forces generated by heaving and pitching foils, in which there is a period of net drag force produced as foils reverse direction at the extremes of the stroke cycle. For example, data on flapping

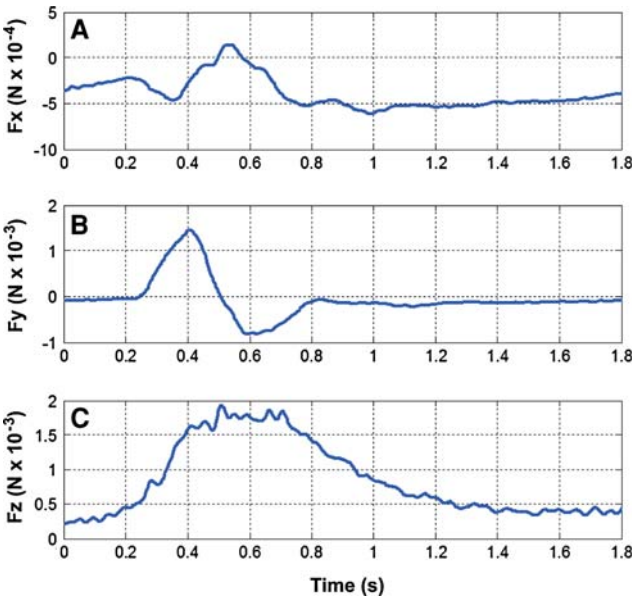

Fig. 9 Wake forces (for one fin) from bluegill sunfish pectoral fin locomotion at 0.5 Ls^{-1} estimated in three dimensions from transverse light sheet stereo PIV data (see Fig. 3c for methods,) calculated by estimating the momentum flux through the transverse light sheet plane, and knowing the weight of the fish. Imaging wake flows at 500 Hz in this plane allows estimation of momentum flux through time. Values should be doubled to estimate total force on the fish from both pectoral fins. There was negligible activity in other fins during this sequence, so total locomotor force on the bluegill can be attributed almost exclusively to the pectoral fins. There is little change in the mean side (**a**) or vertical force (**b**) throughout the fin beat compared to the initial values before the fin beat begins. Small differences in force to the left and right or up and down reflect slight changes in fish position during the fin beat. Note that the pectoral fin generates thrust throughout the fin beat cycle (**c**); there is no time when the pectoral fin produces net drag (negative Fz). Also see Peng et al. (2007), Drucker and Lauder (1999), and Mittal et al. (2006) for other methods of estimating locomotor force from fish pectoral fins

foils by Read et al. (2003), computations of foil thrust coefficients by Dong et al. (2006) and Guglielmini and Blondeaux (2004), all show a time of net drag at stroke reversal. A computational fluid dynamic analysis of the pectoral fin of a wrasse, a fish with a more flapping foil-like fin stroke (Ramamurti et al. 2002), also shows a significant period of drag at the fin reversal, and experimental estimates of thrust coefficients in fishes using flapping and rowing propulsion (Walker and Westneat 2002; Walker 2004) show long periods of drag. In contrast, the data presented here and our previous experimental and computational analyses of the sunfish pectoral fin which exhibits a more complex movement pattern than simple rowing or flapping, shows that thrust is generated throughout the fin beat and that there is no time in the fin beat cycle when net drag is produced (Lauder and Madden 2006; Lauder et al. 2006; Mittal et al. 2006).

Our observation of continuous thrust by the sunfish pectoral fin is understandable in terms of fin kinematics, which contrast with those of rowing and flapping fishes studied previously. Movement of the sunfish pectoral fin, with the cupping shape on the outstroke, the flexible fin surface, the outer third of which is oriented downstream on the outstroke, the wave of bending that passes along the upper third of the fin, area minimization at the transition between downstroke and upstroke, and area expansion on the return stroke, all combine to generate continuous thrust throughout the beat (Fig. 5). Many features of this kinematic pattern are general components of fish fin function (Fish and Lauder 2006; Lauder 2006), and this result suggests that one important role for flexibility of the propulsive fin surface in fishes is to modulate force production and smooth out oscillations that might arise at transitions during the movement cycle. Bending of the fin surface and of individual fin rays allows continued thrust production by at least some portion of the fin at all times during the fin stroke that is sufficient to overcome drag produced by other fin regions.

7 Conclusions and prospectus

The experimental study of fish locomotion has undergone a renaissance in recent decades as new technologies for visualizing fin and body movement and for quantifying water flow produced by the body and fins have matured and become more widely available to biologists. Studying freely swimming fish moving under controlled conditions in laboratory flow tanks has allowed detailed analyses of fin deformation, the role of flexibility in generating propulsive forces, and the forces produced by flexible fins. Fish fins are remarkable in having active camber control and the consequent ability to resist hydrodynamic loading. Furthermore, fin-fin hydrodynamic interactions are substantial, especially among median fins. There are currently no experimental data that suggest an interaction between paired fins and median fins, although such interactions are certainly possible and remain to be demonstrated.

Experimental analyses of living fishes are, by their very nature, limited to studying what nature provides in the way of fin position, structure, and activation pattern. Although surgical modifications of fish fin shape are possible (e.g., Webb 1977), such modifications provide for only a relatively limited range of shape changes, and do not permit major alterations in fin position or movement pattern, and fish may alter the way fins are moved post-surgically. Another approach, and one that allows for much more control over movement pattern and for greater exploration of the parameter space of fin phase, frequency, and amplitude is to use robotic models of fish fins (Kato 1998, 2000; Lauder et al. 2007; Tangorra et al. in press; Triantafyllou and Triantafyllou 1995; Triantafyllou et al. 2004).

Both robotic models of a specific fin type such as the pectoral fin, and the use of more abstract robotic models such as dual-flapping foils to approximate median fin interactions, provide invaluable flexibility for understanding how fish fins function. Analyses of such robotic systems will likely prove to be an important path for future work on fish fin function.

Finally, we anticipate that computational fluid dynamic approaches will increasingly use as input experimentally measured fin kinematics to more accurately estimate locomotor forces, and allow direct comparisons with experimental force measurements. Such studies are, to date, few (but see Akhtar et al. 2007; Mittal 2004; Mittal et al. 2006; Ramamurti et al. 2002). But the promise of a closer integration of computational approaches, the use of robotic models, and increasingly detailed experimental analyses of fish fin function, suggests that the next decade will witness major progress in understanding the function of fish fins, and improved ability to use them to design bio-inspired propulsors for AUVs.

Acknowledgments This work was supported by an ONR-MURI Grant N00014-03-1-0897 on fish pectoral fin function, monitored by Dr. Thomas McKenna and initiated by Dr. Promode Bandyopadhyay, and by NSF grant IBN0316675 to G.V.L. We thank Drs. Rajat Mittal and Promode Bandyopadhyay for many helpful discussions on bio-inspired propulsion. Dr. Wolf Hanke designed the laser scanning system and we are very grateful for his assistance with those experiments. Karsten Hartel and Chris Kenaley kindly provided the grouper photograph in Fig. 1a, Em Standen took the image in Fig. 3a, and Eric Tytell provided the bluegill picture used in Fig. 3c. Tony Julius and Julie Idlet provided invaluable assistance in the lab. Thanks also to two anonymous reviewers who provided comments helpful in clarifying the manuscript.

References

Akhtar I, Mittal R, Lauder GV, Drucker E (2007) Hydrodynamics of a biologically inspired tandem flapping foil configuration. Theor Comput Fluid Dyn 21:155–170

Alben S, Madden PGA, Lauder GV (2007) The mechanics of active fin-shape control in ray-finned fishes. J R Soc Interface 4:243–256

Anderson J (1996) Vorticity control for efficient propulsion. Ph.D. Thesis, MIT/WHOI, 96-02

Brucker C (1997) 3D scanning PIV applied to an air flow in a motored engine using digital high-speed video. Meas Sci Technol 8:1480–1492

Brücker C (2001) Spatio-temporal reconstruction of vortex dynamics in axisymmetric wakes. J Fluid Struct 15:543–554

Burgmann S, Brucker C, Schroder W (2006) Scanning PIV measurements of a laminar separation bubble. Exp Fluids 41:319–326

Carling JC, Williams TL, Bowtell G (1998) Self-propelled anguilliform swimming: simultaneous solution of the two-dimensional Navier-Stokes equations and Newton's laws of motion. J Exp Biol 201:3143–3166

Dickinson MH (2005) The initiation and control of rapid flight maneuvers in fruit flies. Int Comput Biol 45:274–281

Dong H, Mittal R, Najjar FM (2006) Wake topology and hydrodynamic performance of low aspect-ratio flapping foils. J Fluid Mech 566:309–343

Drucker EG, Lauder GV (1999) Locomotor forces on a swimming fish: three-dimensional vortex wake dynamics quantified using digital particle image velocimetry. J Exp Biol 202:2393–2412

Drucker EG, Lauder GV (2000) A hydrodynamic analysis of fish swimming speed: wake structure and locomotor force in slow and fast labriform swimmers. J Exp Biol 203:2379–2393

Drucker EG, Lauder GV (2001a) Wake dynamics and fluid forces of turning maneuvers in sunfish. J Exp Biol 204:431–442

Drucker EG, Lauder GV (2001b) Locomotor function of the dorsal fin in teleost fishes: experimental analysis of wake forces in sunfish. J Exp Biol 204:2943–2958

Drucker EG, Lauder GV (2002a) Experimental hydrodynamics of fish locomotion: functional insights from wake visualization. Int Comput Biol 42:243–257

Drucker EG, Lauder GV (2002b) Wake dynamics and locomotor function in fishes: interpreting evolutionary patterns in pectoral fin design. Int Comput Biol 42:997–1008

Drucker EG, Lauder GV (2003) Function of pectoral fins in rainbow trout: behavioral repertoire and hydrodynamic forces. J Exp Biol 206:813–826

Drucker EG, Lauder GV (2005) Locomotor function of the dorsal fin in rainbow trout: kinematic patterns and hydrodynamic forces. J Exp Biol 208:4479–4494

Fish F, Lauder GV (2006) Passive and active flow control by swimming fishes and mammals. Ann Rev Fluid Mech 38:193–224

Geerlink PJ, Videler JJ (1974) Joints and muscles of the dorsal fin of *Tilapia nilotica* L. (Fam. Cichlidae). Neth J Zool 24:279–290

Geerlink PJ (1979) The anatomy of the pectoral fin in *Sarotherodon niloticus* Trewavas (Cichlidae). Neth J Zool 29:9–32

Geerlink PJ, Videler JJ (1987) The relation between structure and bending properties of teleost fin rays. Neth J Zool 37:59–80

Gibb A, Jayne BC, Lauder GV (1994) Kinematics of pectoral fin locomotion in the bluegill sunfish *Lepomis macrochirus*. J Exp Biol 189:133–161

Guglielmini L, Blondeaux P (2004) Propulsive efficiency of oscillating foils. Euro J Mech B-Fluids 23:255–278

Higham TE, Malas B, Jayne BC, Lauder GV (2005) Constraints on starting and stopping: behavior compensates for reduced pectoral fin area during braking of the bluegill sunfish (*Lepomis macrochirus*). J Exp Biol 208:4735–4746

Jayne BC, Lozada A, Lauder GV (1996) Function of the dorsal fin in bluegill sunfish: motor patterns during four locomotor behaviors. J Morphol 228:307–326

Kato N (1998) Locomotion by mechanical pectoral fins. J Mar Sci Technol 3:113–121

Kato N (2000) Control performance in the horizontal plane of a fish robot with mechanical pectoral fins. IEEE J Oceanic Eng 25:121–129

Kern S, Koumoutsakos P (2006) Simulations of optimized anguilliform swimming. J Exp Biol 209:4841–4857

Lauder GV (2000) Function of the caudal fin during locomotion in fishes: kinematics, flow visualization, and evolutionary patterns. Am Zool 40:101–122

Lauder GV, Drucker EG (2002) Forces, fishes, and fluids: hydrodynamic mechanisms of aquatic locomotion. News Physiol Sci 17:235–240

Lauder GV, Drucker EG (2004) Morphology and experimental hydrodynamics of fish fin control surfaces. IEEE J Oceanic Eng 29:556–571

Lauder GV (2006) Locomotion. In: Evans DH, Claiborne JB (eds) The physiology of fishes, 3rd edn. CRC, Boca Raton, pp 3–46

Lauder GV, Madden PGA (2006) Learning from fish: kinematics and experimental hydrodynamics for roboticists. Int J Automat Comput 4:325–335

Lauder GV, Madden PGA, Mittal R, Dong H, Bozkurttas M (2006) Locomotion with flexible propulsors I: experimental analysis of pectoral fin swimming in sunfish. Bioinsp Biomimet 1: S25–S34

Lauder GV, Tytell ED (2006) Hydrodynamics of undulatory propulsion. In: Shadwick RE, Lauder GV (eds) Fish biomechanics vol 23 in fish physiology. Academic, San Diego, pp 425–468

Lauder GV, Anderson EJ, Tangorra J, Madden PGA (2007) Fish biorobotics: kinematics and hydrodynamics of self-propulsion. J Exp Biol 210 (in press)

Lauder GV, Madden PGA (2008) Advances in comparative physiology from high-speed imaging of animal and fluid motion. Ann Rev Physiol 70 (in press)

Liao J, Lauder GV (2000) Function of the heterocercal tail in white sturgeon: flow visualization during steady swimming and vertical maneuvering. J Exp Biol 203:3585–3594

Liao J, Beal DN, Lauder GV, Triantafyllou MS (2003) The Kármán gait: novel body kinematics of rainbow trout swimming in a vortex street. J Exp Biol 206:1059–1073

Mittal R (2004) Computational modeling in biohydrodynamics: trends, challenges, and recent advances. IEEE J Oceanic Eng 29:595–604

Mittal R, Dong H, Bozkurttas M, Lauder GV, Madden PGA (2006) Locomotion with flexible propulsors II: computational modeling and analysis of pectoral fin swimming in sunfish. Bioinsp Biomimet 1: S35–S41

Müller UK, Stamhuis EJ, Videler JJ (2000) Hydrodynamics of unsteady fish swimming and the effects of body size: comparing the flow fields of fish larvae and adults. J Exp Biol 203:193–206

Nauen JC, Lauder GV (2002a) Hydrodynamics of caudal fin locomotion by chub mackerel, *Scomber japonicus* (Scombridae). J Exp Biol 205:1709–1724

Nauen JC, Lauder GV (2002b) Quantification of the wake of rainbow trout (*Oncorhynchus mykiss*) using three-dimensional stereoscopic digital particle image velocimetry. J Exp Biol 205:3271–3279

Peng J, Dabiri JO, Madden PG, Lauder GV (2007) Non-invasive measurement of instantaneous forces during aquatic locomotion: a case study of the bluegill sunfish pectoral fin. J Exp Biol 210:685–698

Ramamurti R, Lohner R, Sandberg WC (1999) Computation of the 3-D unsteady flow past deforming geometries. Int J Comput Fluid Dyn 13:83–99

Ramamurti R, Sandberg WC, Lohner R, Walker JA, Westneat M (2002) Fluid dynamics of flapping aquatic flight in the bird wrasse: three-dimensional unsteady computations with fin deformation. J Exp Biol 205:2997–3008

Read DA, Hover FS, Triantafyllou MS (2003) Forces on oscillating foils for propulsion and maneuvering. J Fluid Struct 17:163–183

Rockwell D, Magness C, Towfighi J, Akin O, Corcoran T (1993) High image-density particle image velocimetry using laser scanning techniques. Exp Fluids 14:181–192

Shadwick R, Gemballa S (2006) Structure, kinematics, and muscle dynamics in undulatory swimming. In: Shadwick RE, Lauder GV (eds) Fish biomechanics vol 23 in fish physiology. Academic, San Diego, pp 241–280

Standen EM, Lauder GV (2005) Dorsal and anal fin function in bluegill sunfish (*Lepomis macrochirus*): three-dimensional kinematics during propulsion and maneuvering. J Exp Biol 205:2753–2763

Standen EM, Lauder GV (2007) Hydrodynamic function of dorsal and anal fins in brook trout (*Salvelinus fontinalis*). J Exp Biol 210:325–339

Syme DA (2006) Functional properties of skeletal muscle. In: Shadwick RE, Lauder GV (eds) Fish biomechanics vol 23 in fish physiology. Academic, San Diego, pp 179–240

Tangorra JL, Davidson SN, Hunter IW, Madden PGA, Lauder GV, Dong H, Bozkurttas M, Mittal R (in press) The development of a biologically inspired propulsor for unmanned underwater vehicles. IEEE J Oceanic Eng

Triantafyllou MS, Triantafyllou GS (1995) An efficient swimming machine. Sci Am 272:64–70

Triantafyllou MS, Techet AH, Hover FS (2004) Review of experimental work in biomimetic foils. IEEE J Oceanic Eng 29:585–594

Tytell ED (2004) Kinematics and hydrodynamics of linear acceleration in eels, *Anguilla rostrata*. Proc R Soc Lond B 271:2535–2540

Tytell ED, Lauder GV (2004) The hydrodynamics of eel swimming. I. Wake structure. J Exp Biol 207:1825–1841

Tytell ED (2006) Median fin function in bluegill sunfish, *Lepomis macrochirus*: streamwise vortex structure during steady swimming. J Exp Biol 209:1516–1534

Walker JA, Westneat MW (1997) Labriform propulsion in fishes: kinematics of flapping aquatic flight in the bird wrasse *Gomphosus varius* (Labridae). J Exp Biol 200:1549–1569

Walker JA, Westneat M (2002) Kinematics, dynamics, and energetics of rowing and flapping propulsion in fishes. Int Comput Biol 42:1032–1043

Walker JA (2004) Dynamics of pectoral fin rowing in a fish with an extreme rowing stroke: the threespine stickleback (*Gasterosteus aculeatus*). J Exp Biol 207:1925–1939

Warrick DR, Dial KP, Biewener AA (1998) Asymmetrical force production in the maneuvering flight of pigeons. Auk 115:916–928

Webb PW (1977) Effects of median fin amputation on fast-start performance of rainbow trout (*Salmo gairdneri*). J Exp Biol 68:123–135

Wilga CD, Lauder GV (1999) Locomotion in sturgeon: function of the pectoral fins. J Exp Biol 202:2413–2432

Wilga CD, Lauder GV (2000) Three-dimensional kinematics and wake structure of the pectoral fins during locomotion in leopard sharks *Triakis semifasciata*. J Exp Biol 203:2261–2278

Wilga CD, Lauder GV (2001) Functional morphology of the pectoral fins in bamboo sharks, *Chiloscyllium plagiosum*: benthic versus pelagic station holding. J Morphol 249:195–209

Wilga CD, Lauder GV (2002) Function of the heterocercal tail in sharks: quantitative wake dynamics during steady horizontal swimming and vertical maneuvering. J Exp Biol 205:2365–2374

Winterbottom R (1974) A descriptive synonymy of the striated muscles of the Teleostei. Proc Acad Natl Sci Philos 125:225–317

Wolfgang MJ, Anderson JM, Grosenbaugh M, Yue D, Triantafyllou M (1999) Near-body flow dynamics in swimming fish. J Exp Biol 202:2303–2327

Zhu Q, Wolfgang MJ, Yue DKP, Triantafyllou GS (2002) Three-dimensional flow structures and vorticity control in fish-like swimming. J Fluid Mech 468:1–28